

Robust WiFi Localization by Fusing Derivative Fingerprints of RSS and Multiple Classifiers

Xiansheng Guo, *Member, IEEE*, Nkrow Raphael Elikplim, *Student Member, IEEE*, Nirwan Ansari, *Fellow, IEEE*, Lin Li, *Student Member, IEEE*, Lei Wang, *Student Member, IEEE*

Abstract—It is notable that localization accuracy using received signal strength (RSS) fingerprints solely is very vulnerable to dynamic environments. Utilizing multiple fingerprints gleaned from RSS for localization is a propitious strategy to overcome the RSS susceptibility. Brimful utilization via fusing multiple fingerprint functions which supplement each other are not harnessed by existing fusion-based techniques, resulting in low localization accuracy. This paper presents a novel and robust WiFi localization modus operandi by fusing Derivative Fingerprints of RSS with Multiple Classifiers (DIFMIC). DIFMIC first constructs a multiple fingerprints group by gleaned hyperbolic location fingerprint (HLF) and signal strength differences fingerprint (DIFF) from RSS fingerprints. Then, it obtains Multiple Fingerprints Trained Classifiers (MFTCs) via training each basic classifier with each fingerprint. To fully leverage the inherent supplementation among fingerprints and classifiers, a two-layer fusion profiles (weights) joint optimization algorithm with multiple constraints is proposed. We also propose a Fusion Profile Selection (FPS) algorithm to intelligently choose fusion weights from the two-layer fusion profile for a more accurate localization. DIFMIC shows more leverage in combining multiple information, thus exhibiting better robustness in WiFi positioning. Results from our experiments reflect that DIFMIC performs better than other existing methods in real environments.

Index Terms—Indoor Localization, WiFi, Two-layer Fusion Profile, Received Signal Strength (RSS), Fingerprints.

I. INTRODUCTION

LOCATION-Based Services (LBSs) are one of the prominent technologies playing salient roles recently. GPS is applicably used for outdoor positioning and cannot be used in indoor environments due to the obstruction of GPS signals by objects like trees, walls, buildings, leading to an imprecise prediction of device's location and thus triggering further research in indoor positioning [1], [2].

Most of existing WiFi indoor localization methods focused on the single received signal strength (RSS)-based fingerprints because they can be readily derived from some common WiFi devices [3], [4]. However, the inherent drawback of RSS

is its sensitivity to changing environment and heterogeneous hardwares. Channel state impulse (CSI) [5], angle-of-arrival (AOA) [6], time-of-arrival (TOA) [7], and time-difference-of-arrival (TDOA) [8] can also be used for indoor localization, but they all require special hardware support, and are thus not cost-effective. Note that the single fingerprint captures an indoor environment from its own stance, and thus utilizing the single fingerprints is not robust with respect to changing environments.

Machine learning is a propitious strategy to mitigate the drawbacks of the single fingerprint-based localization approaches [6], [9]–[12]. However, most of existing machine-learning-based indoor positioning methods only use single machine learning algorithm as a classifier or regressor, which cannot maximize the merits of machine learning for high accuracy indoor positioning.

To address the above problem, in this paper, we present a novel and robust WiFi localization modus operandi by fusing Derivative Fingerprints of RSS with Multiple Classifiers (DIFMIC), in which a two-layer fusion profile joint optimization algorithm with multiple constraints is proposed. DIFMIC can be deployed on any wireless fingerprints based localization systems without the need for additional sensors like gyroscopes, accelerometers, and magnetometers as well as hardware modifications. We summarize the contributions of this paper as follows:

- 1) A two-layer fusion profile joint optimization algorithm with multiple constraints is proposed in this study. How to choose the related parameters is also addressed to guide DIFMIC implementation. The proposed algorithm can fully leverage the complementarity among Multiple Fingerprints Trained Classifiers (MFTCs). To the best of our knowledge, this is the first work to discuss how to effectively combine multiple sources and multiple machine learning methods simultaneously in a joint optimization framework for indoor positioning.
- 2) Although DIFMIC is validated only by three fingerprints (RSS, hyperbolic location fingerprinting (HLF), and difference fingerprints (DIFF)) and four machine learning methods (K-nearest neighbor (KNN), Random Forest, Naive bayes, and AdaBoost) in this study. It is a generalized fingerprint-based indoor positioning framework and can combine more fingerprints, such as CSI [5], signal strength difference (SSD) [13], and spatial gradient fingerprints [14], and more machine learning methods for more accurate localization guided by ensemble learning theory.

Xiansheng Guo, Nkrow Raphael Elikplim, Lin Li, and Lei Wang are with the Department of Electronic Engineering, University of Electronic Science and Technology of China, Chengdu, 611731 China e-mail: xsguo@uestc.edu.cn, nkrowraph@gmail.com, linli9419@gmail.com, louiewang@foxmail.com.

Nirwan Ansari is with Advanced Networking Lab., the Department of Electrical and Computer Engineering, New Jersey Institute of Technology, Newark, NJ, 07102 USA e-mail: nirwan.ansari@njit.edu.

This work has been supported in part by the National Natural Science Foundation of China under Grant (No. 61371184, No. 61671137, No. 61771114, No. 61771316) and in part by the Application Foundation Projects of Science and Technology Department in Sichuan Province (No. 2018JY0242, No. 2018JY0218).

- 3) A Fusion Profile Selection (FPS) algorithm, which fully exploits MFTCs, is proposed. FPS selects weights from the layers of the fusion network to estimate the final location of a target.

This paper is structured as follows: We introduce some related works in Section II. Our newly proposed DIFMIC localization framework is discussed in Section III. Multiple fingerprints group construction and MFTCs training are analyzed in Section IV. The two-layer fusion profile construction and Fusion Profile Selection (FPS) algorithms in DIFMIC together with the performance analysis of our fingerprints are presented in Section V. Experimental setups and results in two real environments are discussed in Section VI. We finally draw conclusions in Section VII.

II. RELATED WORKS

A. Fingerprints-based WiFi Positioning Techniques

RSS is the most popular fingerprint in WiFi positioning, but it shows severe fluctuation in complex indoor environments. Most recent works like [5], [15] extract CSI to help mitigate the multi-path snag, but they require specialized interface cards (Intel 5300 WiFi cards) which are not readily available in most commodity WiFi. Hossain *et al.* [13] and Kjrgaard *et al.* [16] proposed the signal strength difference (SSD) and HLF fingerprints [16] to overcome the snag of RSS instability from different perspectives. As an alternative to HLF, DIFF [17] was extrapolated from RSS from pairs of APs to solve the variance in signal strengths among heterogeneous devices. Delta-fused principle strength (DFPS) fingerprint was proposed to amalgamate the caliber of fingerprints via combining RSS with delta signal strength (Δ RSS) to revamp positioning accuracy [18]. The spatial gradient fingerprints [14] is also an effective strategy to alleviate the influence of RSS fluctuation without any hardware modification. All the above fingerprints in WiFi positioning can alleviate the fluctuation to some extent from different perspectives. To validate the DIFMIC framework, we use RSS, HLF, and DIFF for simplicity.

B. Fusion-based WiFi Positioning Techniques

Fusion-based WiFi positioning techniques can be categorized into two groups: single measurement-based fusion and multiple measurements-based fusion. Comparatively, the single measurement-based fusion methods mainly resort to the post-processing technology to improve the performance of positioning systems, which is cost-effective. For example, Wang *et al.* [19] proposed a Best Linear Unbiased Estimate (BLUE) method for WiFi localization by fusing the positioning results from distance-based method and machine learning methods only using RSS measurements. Fang *et al.* [9] combined the positioning results from Bayesian approach and neural network model. Fang *et al.* [10] combined the multiple conventional methods, such as Least squares (LS), Multidimensional scaling (MDS), and gradient-based methods, for high accurate localization. Selective Fusion Location Estimation (SELFLOC) [11] can fuse the sources from multiple sources and/or multiple algorithms, but the weights are fixed for positioning environment, and SELFLOC is thus not robust

to changing environments. To overcome the drawbacks, we recently proposed multiple algorithms fusion [20] and multiple measurements fusion [21] methods for WiFi positioning.

In fact, our proposed DIFMIC is a generalized fusion framework which can combine any aforementioned fingerprints and positioning approaches. Furthermore, the WiFi environment is just an application scenario of DIFMIC; DIFMIC can also combine different kinds of fingerprints from the same receivers [6] or different heterogeneous networks [18] with different positioning methods regardless of the adopted machine learning algorithm or traditional method. This paper puts forth essential enhancement by using only RSS fingerprints of WiFi, but additional sensor information from accelerometers and gyroscopes [15], [22]–[24] can be readily incorporated for further improvement.

III. DIFMIC LOCALIZATION FRAMEWORK

A real-world location such as an intramural of a building surrounded by L WiFi APs, is prorated into K grid points. The grids are assigned a unique label. We extract HLF and DIFF from the collected offline RSS samples to obtain our multiple fingerprints group, \mathbf{G} , comprising of RSS, HLF, and DIFF, i.e., $M = 3$. \mathbf{G} can be divided into two groups, namely, $\mathbf{G}' = [\mathbf{G}'_1, \mathbf{G}'_2, \dots, \mathbf{G}'_M] = [\mathbf{D}'_{RSS}, \mathbf{D}'_{HLF}, \mathbf{D}'_{DIFF}]$ and $\mathbf{G}'' = [\mathbf{G}''_1, \mathbf{G}''_2, \dots, \mathbf{G}''_M] = [\mathbf{D}''_{RSS}, \mathbf{D}''_{HLF}, \mathbf{D}''_{DIFF}]$, for training classifiers and constructing our fusion profile, respectively. Here, \mathbf{D}'_{RSS} , \mathbf{D}'_{HLF} , \mathbf{D}'_{DIFF} , \mathbf{D}''_{RSS} , \mathbf{D}''_{HLF} , and \mathbf{D}''_{DIFF} denote the corresponding RSS, HLF and DIFF fingerprints, respectively.

1) *Offline phase:* In the offline phase, we can train the classifiers $f_n(\mathbf{G}'_m)$ by selecting N basic classifiers $f_n(\cdot)$ ($n = 1, 2, \dots, N$) from machine learning methods using \mathbf{G}' , as shown in the upper part of Fig. 1. We refer to a collection of basic classifiers trained with multiple fingerprints as Multiple Fingerprints Trained Classifiers (MFTCs), i.e., $\mathbf{f}(\mathbf{G}') = [f_1(\mathbf{G}'), \dots, f_N(\mathbf{G}')]^T$ with $f_n(\mathbf{G}') = [f_n(\mathbf{G}'_1), f_n(\mathbf{G}'_2), f_n(\mathbf{G}'_3)]^T$. Hence, the number of MFTCs are $MN (= 3N)$. Additionally, we also need to train the two-

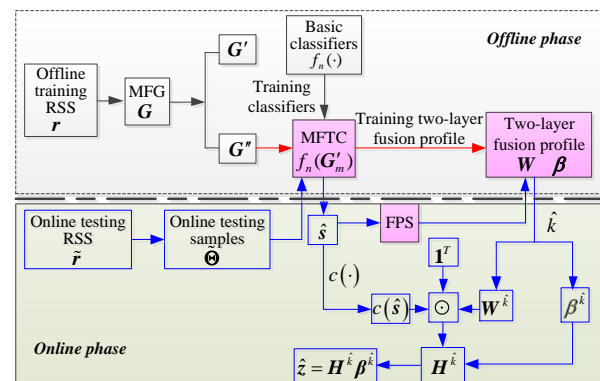


Fig. 1: Architecture of our proposed DIFMIC framework.

layer fusion profile \mathbf{W}^k and β^k using \mathbf{G}'' for each grid point via joint optimization, which will be detailed in Section V. Given the trained MFTCs $f_n(\mathbf{G}'_m)$, the fusion profile \mathbf{W}^k of

the first layer at the k -th grid point in our proposed two-layer fusion framework can be written as

$$\mathbf{W}^k = [\mathbf{w}_1^k, \mathbf{w}_2^k, \dots, \mathbf{w}_N^k], \quad (1)$$

in which $\mathbf{w}_n^k = [w_{1n}^k, w_{2n}^k, \dots, w_{Mn}^k]^T$ is the weights of different classifiers for the n -th fingerprint and $[\cdot]^T$ is the transpose. The fusion profile of the first layer for all K grid points is

$$\mathbf{W} = [\mathbf{W}^1, \mathbf{W}^2, \dots, \mathbf{W}^K]. \quad (2)$$

Similarly, we denote the fusion profile of the second layer at the k -th grid point as

$$\boldsymbol{\beta}^k = [\beta_1^k, \beta_2^k, \dots, \beta_N^k]^T. \quad (3)$$

The fusion profile of the second layer for all K grid points is

$$\boldsymbol{\beta} = [\boldsymbol{\beta}^1, \boldsymbol{\beta}^2, \dots, \boldsymbol{\beta}^K]. \quad (4)$$

2) *Online phase*: Given an online testing RSS vector $\tilde{\mathbf{r}}$ with unknown position, as shown in the lower part of Fig. 1, we first glean HLF $\tilde{\boldsymbol{\eta}}$ and DIFF $\Delta\tilde{\mathbf{r}}$ from $\tilde{\mathbf{r}}$, and obtain the input matrix $\tilde{\boldsymbol{\Theta}} = [\tilde{\boldsymbol{\theta}}_1, \tilde{\boldsymbol{\theta}}_2, \dots, \tilde{\boldsymbol{\theta}}_M]^T = [\mathbf{r}, \boldsymbol{\eta}, \Delta\mathbf{r}]^T$, we can obtain the multiple predictions $\hat{\mathbf{s}} = \mathbf{f}(\tilde{\boldsymbol{\Theta}}, \mathbf{G}') = [f_1(\tilde{\boldsymbol{\Theta}}, \mathbf{G}'), f_2(\tilde{\boldsymbol{\Theta}}, \mathbf{G}'), \dots, f_N(\tilde{\boldsymbol{\Theta}}, \mathbf{G}')]^T$ from MFTCs with $f_n(\tilde{\boldsymbol{\Theta}}, \mathbf{G}')$ being the $M \times 1$ prediction vector of the n -th classifier given the input vector $\tilde{\boldsymbol{\Theta}}$.

Secondly, based on the predictions of MFTC $\hat{\mathbf{s}}$, we need to estimate the grid point \hat{k} from which we can determine the fusion profile $\mathbf{W}^{\hat{k}}$ and $\boldsymbol{\beta}^{\hat{k}}$ for further accurate fusion localization by using our proposed fusion profile selection (FPS) algorithm. After having obtained the fusion profiles $\mathbf{W}^{\hat{k}}$ and $\boldsymbol{\beta}^{\hat{k}}$ of the two-layer fusion network, the outputs of the first layer can be expressed as;

$$\mathbf{H}^{\hat{k}} = [\mathbf{h}_1^{\hat{k}}, \mathbf{h}_2^{\hat{k}}, \dots, \mathbf{h}_N^{\hat{k}}] = \mathbf{1}^T \cdot \mathbf{W}^{\hat{k}} \odot c(\hat{\mathbf{s}}), \quad (5)$$

where \odot denotes the Hadamard product. $\mathbf{1}$ is an $M \times 1$ vector of ones. $c(\cdot) : \mathcal{R}^1 \rightarrow \mathcal{R}^2$ maps a label to a 2-D coordinate. $\mathbf{H}^{\hat{k}}$ is an $2 \times N$ matrix with $\mathbf{h}_n^{\hat{k}} = [x_n, y_n]^T$ being the location estimate of the n -th classifier.

The final location estimate $\hat{\mathbf{z}}$ can be obtained by weighing the fusion profile $\boldsymbol{\beta}^{\hat{k}}$ of the second layer as

$$\hat{\mathbf{z}} = \mathbf{H}^{\hat{k}} \boldsymbol{\beta}^{\hat{k}}, \quad (6)$$

where $\boldsymbol{\beta}^{\hat{k}} = [\beta_1^{\hat{k}}, \beta_2^{\hat{k}}, \dots, \beta_N^{\hat{k}}]^T$.

The key issue for DIFMIC involves: (1) constructing MFTCs $f_n(\mathbf{G}'_m)$; (2) constructing two-layer fusion profiles \mathbf{W} and $\boldsymbol{\beta}$ when several fingerprint functions and fingerprints are given; (3) selecting the optimum fusion profiles $\mathbf{W}^{\hat{k}}$ and $\boldsymbol{\beta}^{\hat{k}}$ in the online testing phase. The intricacies of these three key problems are analyzed in Section V.

IV. MULTIPLE FINGERPRINTS GROUP

A. RSS

Let $r_k^l(t)$ denote the value of RSS from the l -th AP at time index t , and at the k -th grid point. Let $\mathbf{D}'_{RSS}(k)$ denote the U samples of RSS collected at the k -th grid point for basic classifiers training, expressed as:

$$\mathbf{D}'_{RSS}(k) = [\mathbf{r}_k(1), \mathbf{r}_k(2), \dots, \mathbf{r}_k(U)], \quad (7)$$

where $\mathbf{r}_k(u) = [r_k^1(u), r_k^2(u), \dots, r_k^L(u)]^T$, ($u = 1, 2, \dots, U, k = 1, 2, \dots, K$). At all the grid points, The RSS fingerprints for MFTCs training can be expressed as $\mathbf{D}'_{RSS} = [\mathbf{D}'_{RSS}(1), \mathbf{D}'_{RSS}(2), \dots, \mathbf{D}'_{RSS}(K)] \in \mathcal{R}^{L \times U \times K}$.

Similarly, let $\mathbf{D}''_{RSS}(k)$ denote V RSS samples collected at the k -th grid point for the two-layer fusion profiles construction, expressed as:

$$\mathbf{D}''_{RSS}(k) = [\mathbf{r}_k(U+1), \mathbf{r}_k(U+2), \dots, \mathbf{r}_k(U+V)], \quad (8)$$

where $\mathbf{r}_k(v) = [r_k^1(v), r_k^2(v), \dots, r_k^L(v)]^T$, $v = U+1, U+2, \dots, U+V$. So, the RSS fingerprints for fusion profile construction can be expressed as $\mathbf{D}''_{RSS} = [\mathbf{D}''_{RSS}(1), \mathbf{D}''_{RSS}(2), \dots, \mathbf{D}''_{RSS}(K)] \in \mathcal{R}^{L \times V \times K}$.

B. HLF

We denote $\gamma_k^l(t)$ as the converted value of $r_k^l(t)$ to represent the HLF [16] value of a particular time index t , which can be expressed as:

$$\gamma_k^l(t) = 255 + r_k^l(t). \quad (9)$$

Eq. (10) shows the HLF value $\eta_k^{ij}(t)$ at the k -th grid point between the i -th and j -th APs:

$$\eta_k^{ij}(t) = \log\left(\frac{\gamma_k^i(t)}{\gamma_k^j(t)}\right) - \log\left(\frac{1}{\gamma_{\max}}\right), \quad (10)$$

where $\gamma_{\max} = \max\{\gamma_k^1(t), \gamma_k^2(t), \dots, \gamma_k^L(t)\}$, $i \in [1, L-1], j \in [2, L], i < j$. According to Eq. (10), the submatrix $\mathbf{D}'_{HLF}(k)$ can be written as:

$$\mathbf{D}'_{HLF}(k) = [\boldsymbol{\eta}_k(1), \boldsymbol{\eta}_k(2), \dots, \boldsymbol{\eta}_k(U)], \quad (11)$$

where $\boldsymbol{\eta}_k(u) = [\eta_k^{12}(u), \eta_k^{13}(u), \dots, \eta_k^{(L-1)L}(u)]^T$, ($u = 1, 2, \dots, U$). At all grid points, the HLF fingerprints for MFTCs training are expressed as $\mathbf{D}'_{HLF} = [\mathbf{D}'_{HLF}(1), \mathbf{D}'_{HLF}(2), \dots, \mathbf{D}'_{HLF}(K)] \in \mathcal{R}^{Y \times U \times K}$, where $Y = C_2^L$.

Similarly, we can obtain \mathbf{D}''_{HLF} as:

$$\mathbf{D}''_{HLF}(k) = [\boldsymbol{\eta}_k(U+1), \dots, \boldsymbol{\eta}_k(U+V)], \quad (12)$$

where $\boldsymbol{\eta}_k(v) = [\eta_k^{12}(v), \eta_k^{13}(v), \dots, \eta_k^{(L-1)L}(v)]^T$. So, the HLF fingerprints for the two-layer fusion profiles construction are expressed as $\mathbf{D}''_{HLF} = [\mathbf{D}''_{HLF}(1), \mathbf{D}''_{HLF}(2), \dots, \mathbf{D}''_{HLF}(K)] \in \mathcal{R}^{Y \times V \times K}$.

C. DIFF

DIFF [17] is defined for L unique AP pairs at time index t as follows:

$$\Delta r_k^{ij}(t) = r_k^i(t) - r_k^j(t), 1 \leq i < j \leq L. \quad (13)$$

According to Eq. (13), the submatrix $\mathbf{D}'_{DIFF}(k)$ can be expressed for the k -th grid as:

$$\mathbf{D}'_{DIFF}(k) = [\Delta \mathbf{r}_k(1), \Delta \mathbf{r}_k(2), \dots, \Delta \mathbf{r}_k(U)] \quad (14)$$

with $\Delta \mathbf{r}_k(u) = [\Delta r_k^{12}(u), \Delta r_k^{13}(u), \dots, \Delta r_k^{(L-1)L}(u)]^T$, ($u = 1, 2, \dots, U$). The DIFF fingerprints for MFTCs training are expressed as $\mathbf{D}'_{DIFF} = [\mathbf{D}'_{DIFF}(1), \mathbf{D}'_{DIFF}(2), \dots, \mathbf{D}'_{DIFF}(K)] \in \mathcal{R}^{Y \times U \times K}$ at all grid points.

Similarly, we can obtain $\mathbf{D}''_{DIFF}(k)$ as:

$$\mathbf{D}''_{DIFF}(k) = [\Delta \mathbf{r}_k(U+1), \dots, \Delta \mathbf{r}_k(U+V)] \quad (15)$$

with $\Delta \mathbf{r}_k(v) = [\Delta r_k^{12}(v), \Delta r_k^{13}(v), \dots, \Delta r_k^{(L-1)L}(v)]^T$. So, the DIFF fingerprints for the two-layer fusion profiles construction can be written as $\mathbf{D}''_{DIFF} = [\mathbf{D}''_{DIFF}(1), \mathbf{D}''_{DIFF}(2), \dots, \mathbf{D}''_{DIFF}(K)] \in \mathcal{R}^{Y \times V \times K}$.

Now we write our multiple fingerprints group for MFTCs training and fusion profile training as $\mathbf{G}' = [\mathbf{D}'_{RSS}, \mathbf{D}'_{HLF}, \mathbf{D}'_{DIFF}]$ and $\mathbf{G}'' = [\mathbf{D}''_{RSS}, \mathbf{D}''_{HLF}, \mathbf{D}''_{DIFF}]$, respectively. For simplicity, we denote $\mathbf{G}'_1 = \mathbf{D}'_{RSS}$, $\mathbf{G}'_2 = \mathbf{D}'_{HLF}$, and $\mathbf{G}'_3 = \mathbf{D}'_{DIFF}$, $\mathbf{G}''_1 = \mathbf{D}''_{RSS}$, $\mathbf{G}''_2 = \mathbf{D}''_{HLF}$, and $\mathbf{G}''_3 = \mathbf{D}''_{DIFF}$.

D. Multiple Fingerprints Trained Classifiers (MFTCs)

Explicitly, succinctly and contextually, classifiers map a fingerprint to a corresponding label or grid point. Let $f_n(\mathbf{G}')$ represent the n -th classifier ($n = 1, 2, \dots, N$) trained with \mathbf{G}' to map a fingerprint vector to a corresponding label. There are many variants of $f_n(\cdot)$, and any of them can be selected from probabilistic and machine learning models [3], [25]–[27]. In this paper, we select $N = 4$ classifiers, namely, KNN, Random Forest, Naive bayes and AdaBoost to implement DIFMIC. Note that any number and choice of classifiers can be selected to implement DIFMIC.

V. PROPOSED ALGORITHM

A. Two-Layer Fusion Profiles Construction

Our proposed DIFMIC contains two fusion profiles, as illustrated in Fig. 2. The profile of the first layer is designed for the predictions of MFTCs. The outputs of the first layer, denoted as \mathbf{H} , are the temporary positioning results, which will be combined by the fusion profile of the second layer, i.e., β , to estimate the final location. As compared with the existing fusion frameworks using only multiple fingerprints [21] or multiple classifiers [20], the main advantage of our newly proposed two-layer fusion profile is its ability to obtain optimum weights among the MFTCs to achieve better positioning results.

To construct the fusion profiles of the first and second layers in the two-layer fusion localization framework, we input the

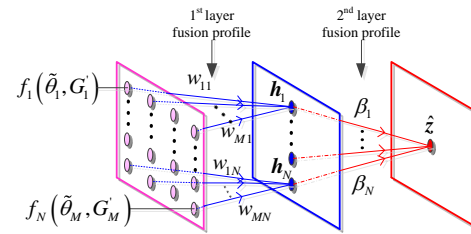


Fig. 2: Two-layer fusion localization framework.

v -th sample from the m -th kind of fingerprint at the k -th grid point, i.e., $\forall \theta_m^k(v) \in \mathbf{G}''$, to the MFTCs, and we can obtain the prediction from the MFTCs as follows

$$\hat{s}_{mn}^k(v) = f_n(\theta_m^k(v), \mathbf{G}'_m), v = U+1, \dots, U+V, \quad (16)$$

where $\hat{s}_{mn}^k(v)$, $n = 1, 2, \dots, N$ is the prediction of the n -th basic classifier trained with the m -th fingerprint, $\theta_m^k(v) \in \mathbf{G}''_m$. Note that at each grid point, we have V offline samples with known location of grid point, so we can obtain V positioning errors.

Given these positioning errors, we propose to construct the fusion profiles of the first and second layers \mathbf{W}^k and β^k by jointly minimizing the mean localization error with weights constraints over the space of all MFTCs as:

$$\begin{aligned} \hat{\mathbf{W}}^k, \hat{\beta}^k = & \arg \min_{\mathbf{W}, \beta} \frac{1}{V} \sum_{v=U+1}^{U+V} e(\hat{\mathbf{z}}^k(v) | \mathbf{W}, \beta) + \frac{\lambda}{V} (\|\mathbf{W}\|_p + \|\beta\|_p) \\ & \text{s.t. } \mathbf{1}^T \mathbf{W} \beta = 1 \\ & a \leq w_{mn} \leq b, m = 1, 2, \dots, M, \\ & a \leq \beta_n \leq b, n = 1, 2, \dots, N, \end{aligned} \quad (17)$$

where $\mathbf{1}$ is an $M \times 1$ vector of ones; $\hat{\mathbf{z}}^k$ is the estimated location given \mathbf{W} and β . The localization error $e(\hat{\mathbf{z}}^k(v) | \mathbf{W}, \beta)$ is given as:

$$e(\hat{\mathbf{z}}^k(v) | \mathbf{W}, \beta) = \|\mathbf{1}^T \mathbf{W} \odot c(\hat{\mathbf{s}}^k(v)) \beta - \mathbf{p}_k\|_2, \quad (18)$$

where $\|\cdot\|_2$ is the ℓ_2 -norm, \odot and $c(\cdot)$ were defined in Eq. (5), $\mathbf{p}_k = [x_k, y_k]^T$ represents the ground truth or known location of the k -th grid point. The prediction vector $\hat{\mathbf{s}}^k(v)$ is given as:

$$\hat{\mathbf{s}}^k(v) = [\hat{s}_{11}^k(v), \dots, \hat{s}_{MN}^k(v)]^T \quad (19)$$

with $\hat{s}_{mn}^k(v)$ being given by Eq. (16). Eq. (17) is a nonlinear optimization problem and can be solved by utilizing the quasi-Newton method. Note that the term $\frac{\lambda}{V} (\|\mathbf{W}\|_p + \|\beta\|_p)$ is a regularization term to prevent over-fitting during the weights training process. The constraint $[a, b]$ helps to reduce the weights training time and $\|\cdot\|_p$ refers to the ℓ_p -norm. The supplementation among diverse kinds of fingerprints and classifiers are explored and excavated by our proposed fusion network. Algorithm 1 wraps up the procedure for constructing our two-layer fusion profiles.

B. Fusion Profile Selection (FPS)

After having obtained the fusion profiles in the offline phase, another hurdle for accurate fusion to ameliorate the

Algorithm 1 Two-layer Fusion Profile Construction

Input: 1) Multiple fingerprints group for fusion profiles construction, $\theta_k^m(v) \in \mathbf{G}_m''$; 2) The number of grid points K ; 3) MFTCs, i.e., $f(\mathbf{G}'')$;
Output: $\hat{\mathbf{W}}$ and $\hat{\beta}$

```

1: for  $k = \{1, 2, \dots, K\}$  do
2:   for  $m = \{1, 2, \dots, M\}$  do
3:     for  $n = \{1, 2, \dots, N\}$  do
4:       for  $v = \{U + 1, M + 2, \dots, U + V\}$  do
5:         Compute the prediction label  $\hat{s}_{mn}^k(v)$  utilizing Eq. (16)
6:         Calculate the localization error using Eq. (18)
7:       end for
8:       Calculate  $\hat{\mathbf{W}}^k$  and  $\hat{\beta}^k$  using Eq. (17)
9:     end for
10:   end for
11: end for
12:  $\hat{\mathbf{W}} = [\hat{\mathbf{W}}^1, \hat{\mathbf{W}}^2, \dots, \hat{\mathbf{W}}^K]$ ,  $\hat{\beta} = [\hat{\beta}^1, \hat{\beta}^2, \dots, \hat{\beta}^K]$ 
13: return  $\hat{\mathbf{W}}$ ,  $\hat{\beta}$ 

```

localization accuracy is selecting the best weights from the two-layer fusion profiles, \mathbf{W}^k and β^k for fusion with the outputs of the MFTCs, for a given online RSS testing sample $\tilde{\mathbf{r}}$. Most previous studies use RSS direct matching method to map the online samples $\tilde{\mathbf{r}}$ with the fingerprints used for training \mathbf{G}'_1 , which decreases localization accuracy in complex environments. To overcome this flaw, FPS offers a fix for this snag. In the offline phase, we select the optimal MFTC by minimizing the localization errors over all K grid points as:

$$(\hat{m}, \hat{n}) = \arg \min_{(m,n)} \sum_{k=1}^K \sum_{v=U+1}^{U+V} \|\mathbf{1}^T \cdot \mathbf{W}^k \odot c(\hat{s}_{mn}^k(v)) \beta^k - \mathbf{p}_k\|_2, \quad (20)$$

where $\hat{s}_{mn}^k(v)$ is given by Eq. (16).

When given a testing RSS sample $\tilde{\mathbf{r}}$ in the online phase, we extract HLF $\tilde{\eta}$ and DIFF $\Delta\tilde{\mathbf{r}}$. For clarity, let $\tilde{\theta}_1 = \tilde{\mathbf{r}}$, $\tilde{\theta}_2 = \tilde{\eta}$ and $\tilde{\theta}_3 = \Delta\tilde{\mathbf{r}}$. With the known index of the optimal MFTC (\hat{m}, \hat{n}) , we can obtain the matching grid point by:

$$\hat{k} = f_{\hat{n}}(\tilde{\theta}_{\hat{m}}, \mathbf{G}_{\hat{m}}''). \quad (21)$$

After having obtained the estimated grid point \hat{k} , we can select the first and second fusion profiles $\hat{\mathbf{W}}_{\hat{k}}$ and $\hat{\beta}_{\hat{k}}$ for more accurate fusion positioning. The final location estimate can be given by Eqs. (5) and (6).

To be laconic, FPS selects the optimal weights by resorting to the optimal MFTC's knowledge, and is thus superior to other fusion-based methods. We summarize the procedure of FPS in Algorithm 2.

C. Robustness of Fingerprints

RSS, DIFF, and HLF fingerprints show different intrinsic characteristics. DIFF and HLF fingerprints adopt different strategies to reduce the impact of hardware heterogeneity. DIFF calculates the differences of the RSS values between

Algorithm 2 Fusion Profile Selection (FPS)

Input: 1) MFTCs, i.e., $f(\tilde{\theta}, \mathbf{G}'')$; 2) $\tilde{\mathbf{r}}$; 3) The fusion profile of the first layer, $\hat{\mathbf{W}}$; 4) The fusion profile of the second layer, $\hat{\beta}$;
Output: The estimated fusion profiles $\hat{\mathbf{W}}^{\hat{k}}$ and $\hat{\beta}^{\hat{k}}$

```

1: Extract  $\Delta\tilde{\mathbf{r}}$  and  $\tilde{\eta}$  from  $\tilde{\mathbf{r}}$ 
2: Find  $\hat{m}$  and  $\hat{n}$  by using Eq. (20)
3: Estimate the grid point  $\hat{k}$  using Eq. (21)
4: Retrieve  $\hat{\mathbf{W}}^{\hat{k}}$  and  $\hat{\beta}^{\hat{k}}$  for the outputs of Algorithm 1
5: return  $\hat{\mathbf{W}}^{\hat{k}}$  and  $\hat{\beta}^{\hat{k}}$ 

```

pairs of APs, while HLF uses ratios of the RSS values between pairs of APs and then normalizes the ratios. Two key metrics, namely, the percentage of standard deviation (PSD) Ψ , and correlation coefficient Φ are defined to show the inherent characteristics of the three fingerprints utilized in this paper. PSD evaluates the ability of a fingerprint against dynamic environment via presenting the statistics at different time index v . The smaller the PSD value for a fingerprint, the more robust the fingerprint. Also, the correlation coefficient evinces the spatial discrimination among grid points. The bigger the Φ , the poorer the spatial discrimination. We define the PSDs of RSS, DIFF, and HLF as:

$$\left\{ \begin{array}{l} \Psi_{k,\text{RSS}}^l = \frac{\sqrt{\frac{1}{U} \sum_{v=1}^U [r_k^l(v) - \mu_r]^2}}{|\mu_r|} \times \% \\ \Psi_{k,\text{DIFF}}^{ij} = \frac{\sqrt{\frac{1}{U} \sum_{v=1}^U [\Delta r_k^{ij}(v) - \mu_{\Delta r}]^2}}{|\mu_{\Delta r}|} \times \% \\ \Psi_{k,\text{HLF}}^{ij} = \frac{\sqrt{\frac{1}{U} \sum_{v=1}^U [\eta_k^{ij}(v) - \mu_{\eta}]^2}}{|\mu_{\eta}|} \times \% \end{array} \right. , \quad (22)$$

where $|\cdot|$ is the absolute value operator. μ_r , $\mu_{\Delta r}$, and μ_{η} denote the mean values of $D'_{\text{RSS}}(k)$, $D'_{\text{DIFF}}(k)$, and $D'_{\text{HLF}}(k)$, respectively.

The correlation coefficient $\Phi(j)$ between the fingerprint vectors at the k -th and $(k+j)$ -th grid points is given as:

$$\left\{ \begin{array}{l} \Phi_{\text{RSS}}(j) = \frac{\mathbf{r}_k^T \mathbf{r}_{k+j}}{\|\mathbf{r}_k\|_2 \|\mathbf{r}_{k+j}\|_2} \\ \Phi_{\text{DIFF}}(j) = \frac{\Delta \mathbf{r}_k^T \Delta \mathbf{r}_{k+j}}{\|\Delta \mathbf{r}_k\|_2 \|\Delta \mathbf{r}_{k+j}\|_2} \\ \Phi_{\text{HLF}}(j) = \frac{\boldsymbol{\eta}_k^T \boldsymbol{\eta}_{k+j}}{\|\boldsymbol{\eta}_k\|_2 \|\boldsymbol{\eta}_{k+j}\|_2} \end{array} \right. . \quad (23)$$

Two different smartphones (Samsung galaxy S7 and Huawei honor 7X) were used to conduct an experiment on how the fingerprints utilized in this paper can handle the hardware heterogeneity problem in the experimental environment defined in Section VI-A. We collected a total of 1750 RSS samples, i.e., 10 samples per grid from the two devices. The mean PSDs of RSS, DIFF and HLF of the two devices are 16.90%, 5.86% and 2.06% respectively. This shows that, DIFF and HLF are more robust than RSS in handling hardware heterogeneity and are very robust to dynamic environments. The mean correlation coefficient for RSS, DIFF and HLF are 0.57, 0.74, and 0.90, respectively. This indicates that, DIFF and HLF performs better than RSS. Table I summarizes the PSD and correlation coefficient for our experiment.

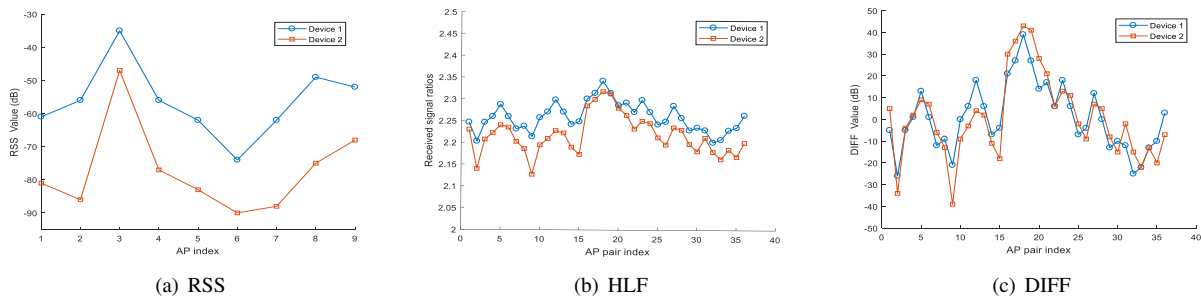


Fig. 3: The RSS, HLF, and DIFF values at the same grid point regarding hardware heterogeneity.

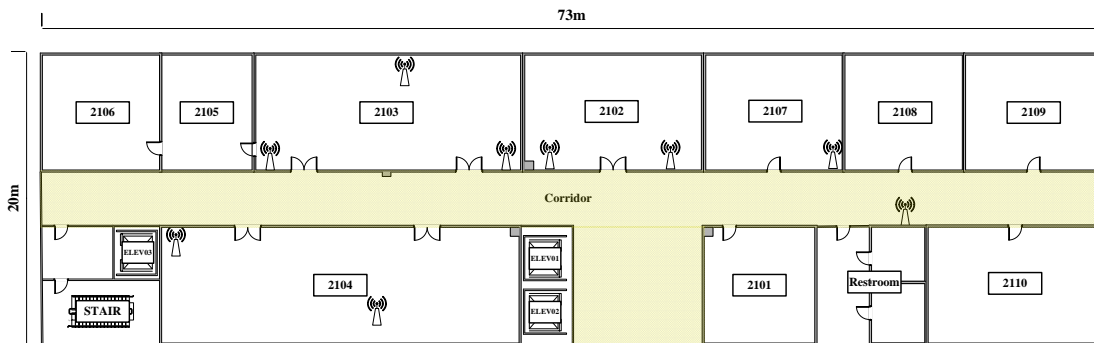


Fig. 4: Floor plan of the office environment.

TABLE I: The percentage of standard deviations and correlation coefficients of different kinds of fingerprints.

metrics	RSS	DIFF	HLF
PSD (Ψ)	16.9%	5.86%	2.06%
correlation coefficient (Φ)	0.57	0.74	0.90

To attest further, we expound how HLF and DIFF fingerprints handle the heterogeneous nature of devices by comparing the mean values of the various fingerprints at the same grid point. Figs. 3(a), 3(b) and 3(c) show the RSS, HLF, and DIFF values at the same grid point. This means that HLF and DIFF can handle the RSS differences among devices from different manufacturers.

To summarize, RSS, HLF, and DIFF have their own pros and cons regarding heterogeneous devices. So, the amalgamation of them by using our proposed DIFMIC can ameliorate positioning accuracy significantly.

VI. EXPERIMENTAL SETUP AND RESULTS

We juxtapose DIFMIC with other fusion-based methods like MMSE [11], DFC [9], DFPS [28], MUCUS [6], WiFi-FAGOT [12] and non-fusion or machine learning methods like KNN, Random Forest, Naive Bayes, and AdaBoost. Two experimental environments are chosen for our test. The first environment is on the 21st floor of the innovation building on the campus of University of Electronic Science and Technology of China, as shown in Fig. 4. The second environment is a university

library with the data collected over a period of 15 months which is publicly available [29]. In each case, the RMSE as defined in Eq. (24) is calculated.

$$\text{RMSE} = \sqrt{\frac{1}{G} \sum_{g=1}^G [(\hat{x}_g - x)^2 + (\hat{y}_g - y)^2]}, \quad (24)$$

where $[x, y]^T$ is the true location or the ground truth, $[\hat{x}_g, \hat{y}_g]^T$ denotes the g -th location estimate, and G is the number fingerprint samples. We perform our simulations on an Intel i5 processor, equipped with 12GB of RAM.

A. Office Environment

This area is 1460 m², i.e., 73m × 20m surrounded by 9 AROCOV 6260 APs [30], with one corridor and 10 offices as shown in Fig. 4. The area is divided into 175 grid points with an interval of 0.8m between adjoining points. $U = 20$ and $V = 10$ RSS samples are collected for G'_1 and G''_1 , respectively with an android smartphone at each grid point. G'_1 and G''_1 are utilized to obtain sets of fingerprints: HLF (G'_2 and G''_2) and DIFF (G'_3 and G''_3). We then train each of our classifiers (KNN, Random Forest, Naive Bayes, and AdaBoost) with RSS and the fingerprints gleaned from RSS to obtain our MFTCs. 975 RSS testing samples in total are collected.

Fig. 5 shows the RMSEs of the various fusion-based algorithms as compared with DIFMIC. The RMSE of MUCUS,

DFC, MMSE, DFPS, KAAL, WIFI-FAGOT and DIFMIC are 6.59, 4.85, 3.59, 3.53, 3.43, 3.32 and 2.50 meters, respectively. These results have validated DIFMIC to be superior over existing fusion-based algorithms, by fully leveraging and supplementing different fingerprint types to improve localization accuracy.

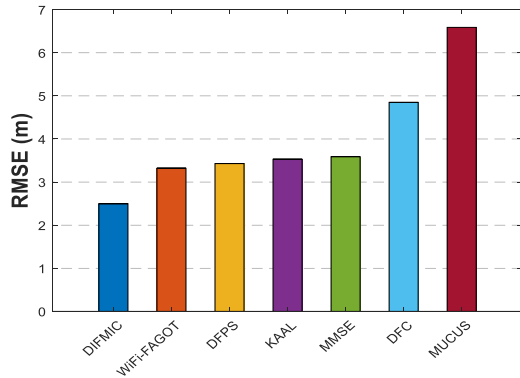


Fig. 5: RMSEs of various fusion-based positioning approaches in the office environment.

Fig. 6 shows the RMSEs of prominent machine learning methods with successive combinations of fingerprints derived from RSSs. It shows that DIFMIC outperforms all successive classifier-fingerprint combinations. The best among the MFTCs is Random Forest with HLF (RF-HLF) pair with RMSE of 3.95 meters followed by Random Forest with RSS (RF-RSS) with RMSE of 3.99 meters. The worst among the MFTCs is Naive Bayes with RSS (NB-RSS) with a RMSE of 4.54 meters. Note that all the MFTCs are fused together with our proposed fusion framework, DIFMIC. This elicits that fusion-based methods yield far better results than utilizing single machine learning algorithms for localization.

Fig. 7 shows the CDFs of the RMSE of DIFMIC juxtaposed with fusion-based methods. It is notable that DIFMIC reduces the 70-th percental of KAAL, DFC, MMSE, MUCUS, DFPS and FAGOT by 24.67%, 37.37%, 23.89%, 49.35%, 18.90% and 18.47%, respectively, indicating that our proposed

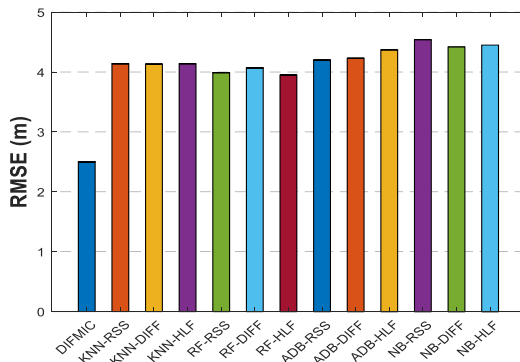


Fig. 6: RMSEs of basic classifier-fingerprint combinations compared with DIFMIC in the office environment.

DIFMIC is better than all previously proposed fusion-based methods.

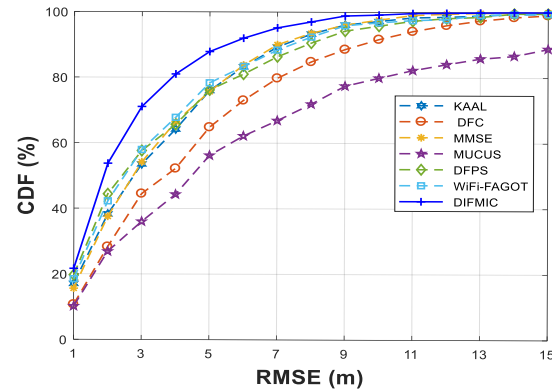
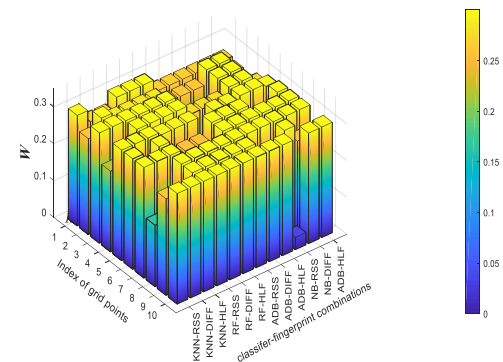
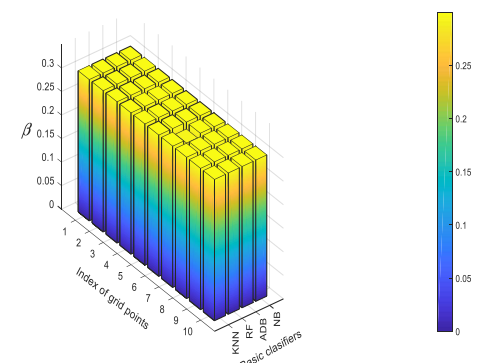


Fig. 7: CDFs of various fusion-based methods juxtaposed with DIFMIC in the office environment.



(a) First layer fusion weights.



(b) Second layer fusion weights.

Fig. 8: Fusion weights of the first and second layers for the first 10 grid points in the office environment.

To throw more light on the weight assignment strategy in the fusion profile regarding fusing multiple classifiers and diverse fingerprints, Fig. 8 shows two 3-D views of the first and second layer weights of our proposed fusion network, for more lucidity for the office testing environment.

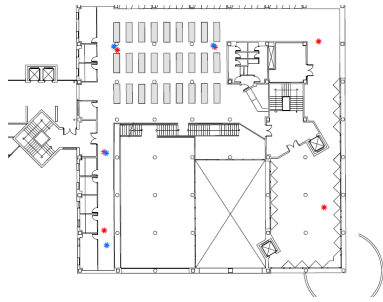


Fig. 9: Floor plan of the library environment. The black asterisks represent the 3rd floor's devices, and black asterisks represent the 5th floor's devices

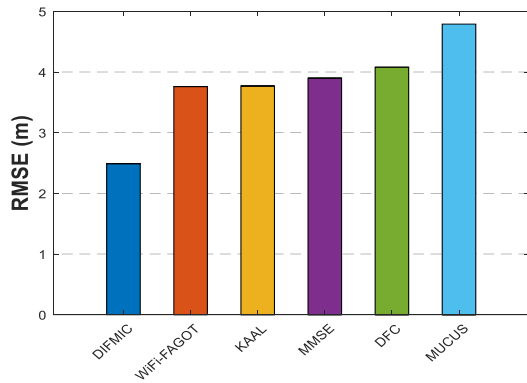


Fig. 10: RMSEs of fusion-based localization methods in the library environment.

B. Library Environment

The publicly available data in [29] were collected over a period of 15 months, with the environment surrounded with 448 APs with 96 grids as indicated in Fig. 9, and can be used as benchmark data for testing localization algorithms. We sample one of the month's training data set, extract HLF and DIFF and use all the data to train our MFTCs. We utilize all the data in another month's test data to test our MFTCs and also to obtain fusion weights. We use all the data in another month's test data for the online phase. We apply the same principles for all the fusion based methods.

Fig. 10 shows the RMSE of DIFMIC as compared to other fusion-based techniques, and shows that DIFMIC outperforms the other fusion based techniques by reporting a RMSE of 2.49m. WiFi-FAGOT, KAAL, MMSE, DFC, and MUCUS incur a RMSE of 3.76m, 3.77m, 3.9m, 4.08m, and 4.79m, respectively. Note that extracting DIFF and HLF increases the dimensionality of the dataset, hence requiring more memory and computational time with the dataset analyzed in the library environment. The dimensions of HLF and DIFF are C_2^L , where L is the number of APs. With the amalgamation of these high dimensional fingerprints, DIFMIC is still able to reduce localization errors better than WiFi-FAGOT, which makes use of RSS, SSD and HLF fingerprints. This shows that DIFMIC performs very well regardless of the dimensionality of the dataset.

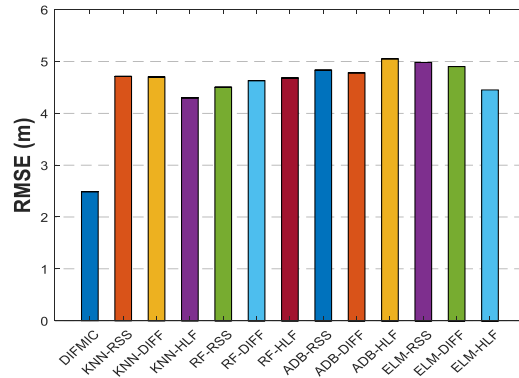


Fig. 11: RMSEs of basic classifier-fingerprint pairs apposed to DIFMIC in the library environment.

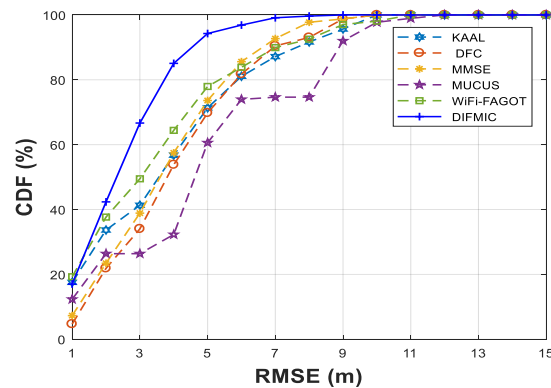


Fig. 12: CDFs of fusion-based methods compared with DIFMIC in the library environment.

Fig. 11 shows the RMSE of DIFMIC apposed with classifier-fingerprint pairs. KNN with HLF (KNN-HLF) has the best RMSE with 4.3 m followed by Random Forest with RSS (RF-RSS) which reports a RMSE of 4.5m. The worst among the basic classifier-fingerprint pairs is AdaBoost with HLF (ADB-HLF) with a RMSE of 5.05m. Note that Naive Bayes was not used in this experiment because of the dimensions of HLF and DIFF fingerprints. It is computationally expensive to train Naive Bayes with high dimensional data, e.g., in this case, HLF and DIFF have dimensions of 576×100128 . This means that any classifier of choice or any number of classifiers can be selected and used to construct DIFMIC with no curtailment. The RMSE of KNN-RSS, KNN-DIFF, RF-RSS, RF-DIFF, RF-HLF, ADB-RSS, ADB-DIFF, ADB-HLF, ELM-RSS, ELM-DIFF and ELM-HLF are 4.71m, 4.70m, 4.5m, 4.63m, 4.68m, 4.83m, 4.78m, 5.05m, 4.98m, 4.9m and 4.45m, respectively. Fig. 12 shows the CDFs of the various fusion based techniques juxtaposed with DIFMIC. DIFMIC reduces the 85th percentile of KAAL, DFC, MMSE, MUCUS and WiFi-FAGOT by 33.27%, 36.73%, 32.44%, 62.04%, and 24.28%, respectively, demonstrating that DIFMIC performs better than other fusion-based methods.

Fig.13 shows the effects of λ , p and the weight constraint parameter, $[a, b]$, during the weights training process and its

- [15] M. Kotaru, K. Joshi, D. Bharadia, and S. Katti, "SpotFi:decimeter level localization using WiFi," *Acm Sigcomm Computer Communication Review*, vol. 45, no. 4, pp. 269–282, 2015.
- [16] M. B. Kjrgaard and C. V. Munk, "Hyperbolic location fingerprinting: A calibration-free solution for handling differences in signal strength," in *Proc. 6th Annu. IEEE Int. Conf. Pervasive Comput. Commun.*, 2008, pp. 110–116.
- [17] F. Dong, Y. Chen, J. Liu, Q. Ning, and S. Piao, "A calibration-free localization solution for handling signal strength variance," in *Proc. Int. Conf. Mobile Entity Local. Tracking GPS-Less Environ.*, 2009, pp. 79–90.
- [18] S. H. Fang and T. N. Lin, "Cooperative multi-radio localization in heterogeneous wireless networks," *IEEE Trans. Wireless Commun.*, vol. 9, no. 5, pp. 1547–1551, 2010.
- [19] L. Wang and W.-C. Wong, "Fusion of multiple positioning algorithms," in *Proc. IEEE Conf. Inf., Commun. Signal Process.*, 2011, pp. 1–5.
- [20] X. Guo, L. Li, N. Ansari, and B. Liao, "Knowledge aided adaptive localization via global fusion profile," *IEEE Internet Things J.*, vol. 5, no. 2, pp. 1081–1089, 2018.
- [21] X. Guo, S. Zhu, L. Li, F. Hu, and N. Ansari, "Accurate WiFi localization by unsupervised fusion of extended candidate location set," *IEEE Internet Things J.*, vol. PP, no. 99, pp. 1–1, 2018.
- [22] S. Kumar, S. Gil, D. Katabi, and D. Rus, "Accurate indoor localization with zero start-up cost," in *Proc. 20th Annu. IEEE Int. Conf. Mobile Comput. Netw.*, 2014, pp. 483–494.
- [23] Z. Yang, C. Wu, Z. Zhou, X. Zhang, X. Wang, and Y. Liu, "Mobility increases localizability: A survey on wireless indoor localization using inertial sensors," *ACM Computing Surveys (Csur)*, vol. 47, no. 3, pp. 1–33, 2015.
- [24] F. Gu, J. Niu, and L. Duan, "Waipo: A fusion-based collaborative indoor localization system on smartphones," *IEEE/ACM Trans. Netw.*, vol. 25, no. 4, pp. 2267–2280, 2017.
- [25] Z. Wu, C. Li, K. Y. Ng, and K. R. P. H. Leung, "Location estimation via support vector regression," *IEEE Trans. Mobile Comput.*, vol. 6, no. 3, pp. 311–321, 2007.
- [26] H. Liu, H. Darabi, P. Banerjee, and J. Liu, "Survey of wireless indoor positioning techniques and systems," *IEEE Trans. Syst., Man, Cybern., Part C*, vol. 37, no. 6, pp. 1067–1080, 2007.
- [27] S. Fang, T. Lin, and K. Lee, "A novel algorithm for multipath fingerprinting in indoor WLAN environments," *IEEE Trans. Wireless Commun.*, vol. 7, no. 9, pp. 3579–3588, 2008.
- [28] S. H. Fang and C. H. Wang, "A novel fused positioning feature for handling heterogeneous hardware problem," *IEEE Trans. Commun.*, vol. 63, no. 7, pp. 2713–2723, 2015.
- [29] G. Mendoza-Silva, P. Richter, J. Torres-Sospedra, E. Lohan, and J. Huerta, "Long-term WiFi fingerprinting dataset for research on robust indoor positioning," vol. 3, no. 1, pp. 1–17, 2018.
- [30] AP6260, "Airocov," <http://www.airocov.com/airocov/Home/View/gw/porduce/porduce6260.html>.



Xiansheng Guo (S'07–M'11) received the B.Eng. degree from Anhui Normal University, Wuhu, China, in 2002, the M.Eng. degree from Southwest University of Science and Technology, Mianyang, China, in 2005, and the Ph.D. degree from the University of Electronic Science and Technology of China (UESTC), Chengdu, China, in 2008. From 2008 to 2009, he was a Research Associate in the Department of Electrical and Electronic Engineering, University of Hong Kong. From 2012 to 2014, he was a Research Fellow in the Department of Electronic

Engineering, Tsinghua University. He is currently an Associate Professor in the Department of Electronic Engineering, UESTC. From 2016 to 2017, he was a research scholar in Advanced Networking Laboratory, Department of Electrical and Computer Engineering, New Jersey Institute of Technology, Newark, NJ, USA. His research interests include array signal processing, wireless localization, machine learning, transfer learning, information fusion, and software radio design.



Nkrow Raphael Elikplim received a B. Sc. degree in Computer Science from Kwame Nkrumah University of Science and Technology, Ghana in 2014. He is currently pursuing a master degree in Information and Communication Engineering at the university of Electronic Science and Technology of China (UESTC), Chengdu, China.

His research areas are Machine Learning, information fusion and Indoor localization. He also has three years working experience in the telecommunication industry.



Nirwan Ansari (S'78–M'83–SM'94–F'09) received a Ph.D. from Purdue University, an MSEE from the University of Michigan, and a BSEE (summa cum laude with a perfect GPA) from NJIT. He is Distinguished Professor of Electrical and Computer Engineering at the New Jersey Institute of Technology (NJIT). He has also been a visiting (chair) professor at several universities.

He authored *Green Mobile Networks: A Networking Perspective* (Wiley-IEEE, 2017) with T. Han, and co-authored two other books. He has also (co-

authored more than 600 technical publications, over 250 published in widely cited journals/magazines. He has guest-edited a number of special issues covering various emerging topics in communications and networking. He has served on the editorial/advisory board of over ten journals. His current research focuses on green communications and networking, cloud computing, drone-assisted networking, and various aspects of broadband networks.

He was elected to serve in the IEEE Communications Society (ComSoc) Board of Governors as a member-at-large, has chaired some ComSoc technical and steering committees, has been serving in many committees such as the IEEE Fellow Committee, and has been actively organizing numerous IEEE International Conferences/Symposia/Workshops. He has frequently been delivering keynote addresses, distinguished lectures, tutorials, and invited talks. Some of his recognitions include several Excellence in Teaching Awards, a few best paper awards, the NCE Excellence in Research Award, the ComSoc TC-CSR Distinguished Technical Achievement Award, the ComSoc AHSN TC Technical Recognition Award, the IEEE TCGCC Distinguished Technical Achievement Recognition Award, the NJ Inventors Hall of Fame Inventor of the Year Award, the Thomas Alva Edison Patent Award, Purdue University Outstanding Electrical and Computer Engineering Award, NCE 100 Medal, and designation as a COMSOC Distinguished Lecturer. He has also been granted 38 U.S. patents.



Lin Li (S'12) received the B.Eng. degree from University of Electronic Science and Technology of China (UESTC), Chengdu, China, in 2016. He is now working toward the Ph.D. degree in the department of Information and Communication Engineering, UESTC.

His research interests include indoor localization, machine learning, and transfer learning.



Lei Wang (S'14) received the B.Eng. degree from the Jilin University, Changchun, China, in 2018. He is currently pursuing the masters degree in Information and Communication Engineering at the university of Electronic Science and Technology of China, Chengdu, China.

His current research interests include indoor localization, machine learning and transfer learning.